TISSUE ENGINEERING: Part A
Volume 27, Numbers 11 and 12, 2021

DOI: 10.1089/ten.tea.2020.0278

termis
Tissue Engineering
& Regenerative Medicine
International Society

ORIGINAL ARTICLE

Matrix Control of Periodontal Ligament Cell Activity Via Synthetic Hydrogel Scaffolds

David Fraser, DDS, MS,[1,2] Tram Nguyen,[3] and Danielle S.W. Benoit, PhD[3–7]

Rebuilding the tooth-supporting tissues (periodontium) destroyed by periodontitis remains a clinical challenge. Periodontal ligament cells (PDLCs), multipotent cells within the periodontal ligament (PDL), differentiate and form new PDL and mineralized tissues (cementum and bone) during native tissue repair in response to specific extracellular matrix (ECM) cues. Thus, harnessing ECM cues to control PDLC activity *ex vivo*, and ultimately, to design a PDLC delivery vehicle for tissue regeneration is an important goal. In this study, poly(ethylene glycol) hydrogels were used as a synthetic PDL ECM to interrogate the roles of cell–matrix interactions and cell-mediated matrix remodeling in controlling PDLC activity. Results showed that PDLCs within matrix metalloproteinase (MMP)-degradable hydrogels expressed key PDL matrix genes and showed a six to eightfold increase in alkaline phosphatase (ALP) activity compared with PDLCs in nondegradable hydrogel controls. The increase in ALP activity, commonly considered an early marker of cementogenic/osteogenic differentiation, occurred independent of the presentation of the cell-binding ligand RGD or soluble media cues and remained elevated when inhibiting PDLC-matrix binding and intracellular tension. ALP activity was further increased in softer hydrogels regardless of degradability and was accompanied by an increase in PDLC volume. However, scaffolds that fostered PDLC ALP activity did not necessarily promote hydrogel ECM mineralization. Rather, matrix mineralization was greatest in stiffer, MMP-degradable hydrogels and required the presence of soluble media cues. These divergent outcomes illustrate the complexity of the PDLC response to ECM cues and the limitations of current scaffold materials. Nevertheless, key biomaterial design principles for controlling PDLC activity were identified for incorporation into scaffolds for periodontal tissue regeneration.

Keywords: tissue engineering, hydrogels, periodontal ligament cells, periodontitis

Impact Statement

Engineered scaffolds are an attractive approach for delivering periodontal ligament cells (PDLCs) to rebuild the tooth-supporting tissues. Replicating key extracellular matrix (ECM) cues within tissue engineered scaffolds may maximize PDLC potential. However, the identity of important ECM cues and how they can be harnessed to control PDLC activity is still unknown. In this study, matrix degradability, cell–matrix binding, and stiffness were varied using synthetic poly(ethylene glycol) hydrogels for three-dimensional PDLC culture. PDLCs exhibited dramatic and divergent responses to these cues, supporting further investigation of ECM-replicating scaffolds for control of PDLC behavior and periodontal tissue regeneration.

[1]Translational Biomedical Science, University of Rochester, Rochester, New York, USA.
[2]Eastman Institute for Oral Health, University of Rochester, Rochester, New York, USA.
Departments of [3]Biomedical Engineering and [4]Chemical Engineering, University of Rochester, Rochester, New York, USA.
[5]Materials Science Program, University of Rochester, Rochester, New York, USA.
[6]Center for Oral Biology, University of Rochester, Rochester, New York, USA.
[7]Center for Musculoskeletal Research, University of Rochester, Rochester, New York, USA.

Introduction

THE PERIODONTIUM IS a group of teeth-supporting tissues in which the periodontal ligament (PDL) plays a key role. In particular, the PDL transmits forces between the tooth and adjacent tissues through a collagen fiber network spanning the PDL and inserting into both cementum, a thin mineralized tissue that lines the tooth root, and the alveolar bone.[1] The PDL is highly vascularized and cellular, containing fibroblasts that remodel and maintain the PDL, as well as populations of cementoblasts and osteoblasts.[2] A distinct cell population resides adjacent to PDL blood vessels.[3,4] Upon injury to the periodontium, these periodontal ligament cells (PDLCs) proliferate, migrate from the PDL, and differentiate to supply a pool of tissue-regenerative cementoblasts, fibroblasts, and osteoblasts.[5–7]

The PDL, along with cementum and alveolar bone, is lost as a result of periodontitis, a chronic and widespread disease characterized by a destructive host immune response to persistent bacterial biofilms.[8] Rebuilding the supporting alveolar bone along with guiding the formation of new cementum and interposed PDL is a significant clinical challenge with current therapies utilizing grafting materials, selective cell repopulation, and/or growth factors. Unfortunately, these efforts show only limited success.[9,10] An emerging regenerative approach is periodontal tissue engineering, wherein cells and scaffolds are assembled *ex vivo* and transplanted to reconstruct the previously destroyed tissues.[11]

PDLCs are an attractive regenerative cell for periodontal tissue engineering. Cultured PDLCs have stem cell properties, including self-renewal, *in vitro* plasticity, and the ability to form cementum and bone when transplanted *in vivo*.[12–14] Furthermore, transplanted PDLCs show greater potential for fostering periodontal tissue regeneration compared with cells derived from bone or gingiva.[15–17] Despite this promise, current scaffolds are limited in their ability to promote transplanted PDLC survival and proliferation while maintaining control over PDLC phenotype.[18,19]

The PDL extracellular matrix (ECM) transmits both the biophysical and biochemical cues responsible for PDLC activation, migration, and differentiation.[20,21] Replicating these cues within an engineered ECM may enable control over PDLC behavior and lead to development of a biomaterial for predictable periodontal tissue regeneration. To this end, hydrogels are commonly used as a matrix mimetic to control cell activity and deliver cells and regenerative factors to tissue defects.[22,23] Previous work has confirmed the integral roles of two ECM cues for directing bone marrow stromal cell (BMSC) differentiation and bone formation within covalently crosslinked hydrogels: matrix metalloproteinase (MMP)-mediated matrix degradation and presentation of integrin binding domains.[24–26] However, the role of PDLC–matrix interactions in determining PDLC phenotype are largely unknown. The unique PDLC niche (the PDL) and the distinct *in vivo* behavior of transplanted PDLCs further motivates the design and testing of scaffolds for PDLC culture and delivery.[12,15]

In this study, poly(ethylene glycol) (PEG) hydrogels were used as a synthetic ECM functionalized with peptides to enable MMP-mediated matrix degradation and/or PDLC integrin-matrix binding. PEG was chosen as the hydrogel polymer as it lacks inherent bioactivity but has well-defined chemistries that allow for precise introduction of cell-responsive and instructive components.[27] Furthermore, PEG hydrogels can be conveniently formed by thiol-norbornene step-growth polymerization, a process that is highly cytocompatible and enables facile incorporation of thiol-containing polymers and/or peptides.[28] PDLC survival and phenotype within PEG hydrogels was explored as a function of MMP degradability, adhesive ligand functionalization, and matrix density over 3 weeks of *in vitro* culture with the overall aim of identifying the role of these ECM cues in controlling PDLC activity.

Methods

PEG macromer synthesis

8-arm PEG (20 kDa) was obtained from JenKem Technology USA. PEG-dithiol (2 kDa) was purchased from Laysan Bio, Inc., 5-norbornene-2-carboxylic acid (norbornene), *N*,*N*′-dicyclohexylcarbodiimide (DCC), and 4-dimethylaminopyridine (DMAP) were purchased from Alfa Aesar. All other materials were obtained from Fisher Scientific unless specified otherwise.

8-arm PEG-norbornene was synthesized using established methods.[28,29] In brief, 20 g PEG-hydroxyl was dissolved in 25 mL dichloromethane (DCM) with pyridine (5 meq per PEG arm) and DMAP (0.5 meq) under nitrogen. In a separate vessel, norbornene (10 meq) and DCC (10 meq) were dissolved in 100 mL DCM. The PEG solution was added dropwise to the vessel containing norbornene that was then purged with nitrogen and left to react overnight at room temperature. The following day, 8-arm PEG-norbornene was filtered to remove excess norbornene salts and then precipitated in ice-cold diethyl ether. PEG-norbornene solids were dissolved in chloroform and washed in ether, with the process repeated twice. Percent functionalization of PEG arms with norbornene was determined with ^{1}H-NMR ($CDCl_3$): $\delta = 6.0–6.3$ ppm (norbornene vinyl protons, 8H, multiplet), 3.5–3.9 ppm (PEG ether protons, 1818H, multiplet). PEG-norbornene macromers with functionalization ≥90% were dialyzed against water for 72 h (1000 Da molecular weight cutoff [MWCO]; Spectrum Labs), lyophilized, and stored at −20°C until used in experiments.

Peptide synthesis

The peptide ligands RGD (CGRGDSG) and scrambled (Scr, CGRDGSG) were synthesized using solid-phase peptide synthesis (Liberty 1 Microwave-Assisted Peptide Synthesizer, CEM) on FMOC-Gly-Wang resin (Novabiochem). Amino acids (AAPTEC) were dissolved in *N*-methyl-2-pyrrilidone (NMP; Oakwood Chemical) at 0.2 M. 0.5 M 2-(1H-Benzotriazole-1-yl)-1,1,3,3-tetramethyluronium hexafluorophosphate (AnaSpec) in dimethylformamide (DMF; Fisher Scientific) was used as an activator, and 2 M *N*-ethyldiisopropylamine (Alfa Aesar) in NMP was used as the activator base. Deprotection was performed with 5% piperazine (Alfa Aesar) in DMF. Peptides were cleaved for 2 h in a cocktail consisting of 0.5 mL triisopropylsilane, 0.5 mL ddH_2O, 0.5 mL 3,6 dioxa-1,8-octane dithiol, and 18.5 mL trifluoracetic acid. Cleaved peptides were precipitated and washed in ether and vacuum-dried overnight.

Peptide molecular mass was verified using matrix-assisted desorption/ionization-time of flight. Peptides were dialyzed against ddH_2O for 24 h (500 MWCO) and lyophilized. Peptide aliquots were made by dissolving peptide in Dulbecco's phosphate-buffered saline (PBS; Gibco) and stored at −80°C. Aliquots were tested to determine the concentration of dissolved peptide by measuring absorbance at 205 nm on an Evolution™ UV-Vis detector (Thermo Scientific).[30] The concentration of free thiols present in peptide aliquots was determined using Ellman's reagent (Fisher Scientific) using a L-cysteine (Alfa Aesar) standard curve in a 0.1 M sodium phosphate buffer with 1 mM ethylenediaminetetraacetic acid (EDTA; pH 8.0), with absorbance read at 412 nm using a Cytation 5 plate reader (Biotek Instruments).

The MMP-degradable peptide crosslinker GKKCGPQG IWGQCKKG was purchased from Genscript, dissolved in PBS, and stored at −80°C. Aliquots were tested for free thiols before use with Ellman's reagent as described above.

Hydrogel formation and characterization

PEG macromer solutions consisted of 8-arm PEG-norbornene, either a nondegradable (PEG-dithiol, nondegradable [ND]) or MMP-degradable peptide (MMP) crosslinker, 2 mM of either RGD or Scr peptide, and 0.05 wt% photoinitiator lithium phenyl-2,4,6-trimethylbenzoyl phosphinate (LAP), all in PBS (Fig. 1A–D). LAP was synthesized as previously described.[31] Both crosslinkers were used at substochiometric ratios to PEG (thiol:norbornene ratio 0.6:1) to provide norbornene sites for peptide ligand incorporation (RGD or Scr) while maintaining similar mechanical properties across all conditions. One milliliter syringes with tips removed were used as hydrogel molds, with each mold receiving 30 μL PEG macromer solution. Hydrogels were formed using long-wave ultraviolet (UV) light ($\sim$5 mW/cm^2, 365 nm) for 3 min and transferred to PBS for 24 h before characterization.

Hydrogels underwent mechanical testing by unconfined compression using a Q-Test/5 materials test frame with a 5 N load cell (MTS) to determine Young's modulus. Hydrogel mesh size was estimated using the mass of hydrogels at equilibrium swelling and after lyophilization as previously described.[32]

PDLC isolation and culture

PDLCs were isolated from extracted human third molars after patient consent (University of Rochester approved protocol RSRB00072932). Immediately after extraction, teeth were placed in a collection buffer consisting of Hanks' balanced salt solution (Gibco) with 5% fetal bovine serum (FBS; Atlanta Biologicals), 100 U/mL penicillin, 100 mg/mL streptomycin, and 0.25 μg/mL amphotericin B (1× antibiotic-antimycotic; Gibco). A scalpel blade was used to remove PDL tissue from the middle third of each root and to mince tissue into pieces <0.5 mm in diameter. PDL fragments were rinsed 2× in collection buffer and transferred to a digestion buffer composed of collagenase type 1 (900 U/mL; Gibco) and dispase type II (2.3 U/mL; Sigma) in PBS and incubated at 37°C for 1 h. An excess of collection buffer was added to digestion buffer and the digest was passed through a 70 μm cell strainer to produce a single-cell suspension of PDLCs. The PDLC suspension was centrifuged at 400 *g* for 10 min, resuspended in growth medium (minimum essential medium α [α-MEM] with nucleosides and Glutamax [Gibco], 20% FBS, and 1× antibiotic-antimycotic [Gibco]), and plated in six-well plates at a density of 1000 nucleated cells/cm^2. Culture medium was changed at 24 h to remove nonadherent cells and then changed twice weekly until adherent PDLCs reached 80% confluence. PDLCs were detached using 0.05% Trypsin with EDTA (Gibco), seeded into T-75 flasks and grown until 80% confluence before passaging. PDLCs at passage 3 were characterized and PDLCs from passages 3 to 6 were used for all experiments. PDLC surface marker expression and differentiation capability were tested before hydrogel encapsulation using established methods.[33]

PDLC encapsulation and culture

PEG macromer solutions were prepared as described previously. 6×10^4 freshly passaged PDLCs were suspended in 30 μL macromer solution, pipetted into cylindrical syringe molds, and formed under UV light for 3 min. Each hydrogel construct (diameter 4.5 mm, height 2 mm) was transferred to one well in a 48-well plate containing 0.5 mL basal medium (α-MEM, 10% FBS) and allowed to equilibrate for 24 h. Hydrogels were then transferred to new wells containing fresh basal or cementogenic/osteogenic (inductive) medium (α-MEM with 10% FBS, 100 μM L-ascorbate 2-phosphate, 10 mM β-glycerophosphate, and 100 nM dexamethasone). Culture media was changed 2–3 times per week.

For experiments using soluble RGD (sol RGD), PDLCs were incubated with 0.5 mM RGD peptide (RGDS; Bachem) for 30 min before encapsulation, then fresh medium containing 0.5 mM sol RGD was added daily. For rho-associated protein kinase (ROCK) inhibition, 10 μM Y-27632 (Tocris) was added to culture medium immediately after encapsulation and then daily for 7 days.

PDLC viability and morphology

Hydrogel constructs were removed from basal medium at specified time points, rinsed once in PBS, and incubated with 4 μM ethidium homodimer-1 and 2 μM calcein AM (Invitrogen) in PBS for 30 min at 37°C, then rinsed 2× with PBS. Each hydrogel was transferred to a glass-bottomed dish (Mattek) and imaged at 10× magnification using a confocal microscope (Olympus FV1000). Single z-stack images were acquired at 100 μm intervals spanning the entire interior of each hydrogel (excluding the top and bottom hydrogel surfaces). ImageJ software was used to count the total number of live or dead cells and to determine the mean cell aspect ratio of each live cell image. Aspect ratio was calculated as the mean cell major axis divided by the mean minor axis with values increasing with more spread cells. Percent live cells and mean aspect ratio was calculated for each z-stack image within each hydrogel and then z-stack image mean values were averaged together to produce a whole hydrogel value.

PDLC proliferation

Hydrogel constructs were equilibrated in basal medium for 24 h postpolymerization before transferring to fresh basal medium with 10% alamarBlue (Invitrogen) for 21 h. Constructs were then removed and placed in fresh basal

medium, and the culture medium with alamarBlue was transferred to 96-well plates to read fluorescence at 560/590 nm. This process was repeated for each construct at 1, 2, and 3 weeks after polymerization. Relative fluorescent units (RFU) for each construct at each time point was normalized to the RFU of the same construct at 24 h to calculate the relative cell number.

RNA extraction, reverse transcription, and quantitative polymerase chain reaction

Each hydrogel was removed from culture, rinsed with PBS, and transferred to a 1.5 mL centrifuge tube containing 350 μL TRK lysis buffer (Omega Bio-Tek) and 7 μL β-mercaptoethanol (VWR). Hydrogels were homogenized in lysis buffer using polypropylene pellet pestles for 45 s and centrifuged at 18,000 *g* for 3 min. Supernatant from two hydrogels was combined and passed through homogenizer columns (Omega), followed by addition of ethanol to precipitate RNA. Samples were then transferred to E.Z.N.A.® (Omega) columns for RNA isolation, on-column DNA digestion, and purification. RNA concentration was measured using a Nano-Vue™ UV-Vis spectrophotometer (GE Healthcare). Two hundred fifty nanograms RNA per sample was reverse transcribed using iScript™ cDNA synthesis kit (BioRad). Quantitative polymerase chain reaction was performed custom primers (Supplementary Table S1) and PowerUp™ SYBR™ green mastermix at an annealing temperature of 60°C. The Pfaffl method was used to calculate relative gene expression using *RPL32* as the housekeeping gene.[34]

Alkaline phosphatase activity

After 1 or 2 weeks culture in basal or inductive medium, hydrogel were rinsed in PBS, transferred to 1.5 mL centrifuge tubes containing 200 μL RIPA buffer (150 mM NaCl, 1% Nonidet™ p-40 substitute, 0.5% sodium deoxycholate, 0.1% sodium dodecyl sulfate, and 25 mM Tris-HCl in ddH_2O), and homogenized using polypropylene pellet pestles for 45 s. Two hundred microliters of additional RIPA buffer was added to the tubes that were then centrifuged for 5 min at 18,000 *g*. The supernatant was used to quantify alkaline phosphatase (ALP) activity and to detect the concentration of DNA in each sample. For ALP activity, *p*-nitrophenyl phosphate (PNPP) tablets (Fisher Scientific) were dissolved in a diethanolamine buffer (1.0 M diethanolamine in ddH_2O with 0.5 mM $MgCl_2$, pH 9.8) at a concentration of 1 mg/mL. Cell lysate was incubated with an equivalent volume of PNPP in buffer, and absorbance (405 nm) was read every minute for 10 min. ALP concentration was determined based on the slope of absorbance over time using calf intestinal ALP (Promega) as the standard.[35] ALP activity was normalized to DNA content for each hydrogel that was determined using PicoGreen™ reagent (Invitrogen).

Whole hydrogel ALP and immunocytochemical staining

Hydrogel constructs were removed from culture, rinsed in PBS, fixed in 4% paraformaldehyde for 30 min, then rinsed 2× in PBS. Whole hydrogels stained for ALP activity were incubated in nitro-blue tetrazolium chloride/5-bromo-4-chloro-3′-indolyphosphate p-toluidine salt (NBT/BCIP, Thermo Scientific) for 45 min then rinsed 3× in PBS before imaging with a digital camera (Canon Rebel T4i). Hydrogels stained for ECM proteins were blocked in 5% bovine serum albumin (BSA; Roche) with 0.1% Triton X-100 (Sigma) in PBS for 1 h at room temperature and then incubated overnight with antibodies against collagen type 1 (COL1) and periostin (POSTN) at 4°C (see Supplementary Table S2 for all antibodies). Hydrogels were then rinsed three times in 3% BSA with 0.05% Triton X-100 for 45 min each followed by incubation with fluorescent secondary antibody and Alexa Fluor® 568 phalloidin (Invitrogen) overnight in 5% BSA with 0.1% Triton X-100. Hydrogels were then rinsed 3× in PBS, incubated with 500 nM 4′,6-diamidino-2-phenylindole (DAPI; Invitrogen) for 1 h, rinsed 3× in PBS, and stored at 4°C until imaged. Hydrogels were placed in glass bottom dishes and imaged on a confocal microscope (Olympus FV1000). Hydrogels stained with only secondary antibodies were used as control to confirm primary antibody specificity.

PDLC volume and sphericity analysis

Hydrogels were cultured in basal medium for 1 week, fixed, and stained with Alexa Fluor® 568 phalloidin and DAPI as described previously. Images were acquired from within 150 μm of the hydrogel surface using a confocal microscope (Olympus FV1000) equipped with a 60× water immersion objective (UPLSAPO60XW, NA 1.2) using a step size of 0.28 μm with *x*, *y* resolution of 0.103 and 0.103 μm. Imaris 9.6 software was used to automatically threshold PDLC surfaces and calculate PDLC volume and surface area. A minimum of 10 cells per hydrogel were analyzed, excluding cells in contact with other cells or on the hydrogel surface. Sphericity was calculated using the formula $\frac{\pi^{1/3}(6V)^{2/3}}{A}$ where V is cell volume and A is cell surface area. Cells with sphericity values approaching 1 are more spherical, whereas cells with sphericity closer to 0 are more linear.

ECM mineralization

After 3 weeks of culture in basal or inductive medium, constructs were transferred into 48-well plates with each well containing 500 μL of 2 mM xylenol orange (Sigma-Aldrich) in culture medium and incubated overnight at 37°C to label calcium deposits in the PEG hydrogel.[36,37] Hydrogels were then rinsed in fresh medium followed by incubation in PBS with 5 μg/mL Hoechst 33342 (Invitrogen) for 15 min to label cell nuclei. Hydrogels were rinsed 2× in PBS then imaged in glass-bottomed dishes using a confocal microscope (Olympus FV1000). Images were acquired at 10× magnification and processed in ImageJ as described previously. A series of images was taken in each hydrogel at 100 μm intervals. For each z-stack image, the total xylenol orange positive area was divided by the number of Hoechst-stained nuclei to give a normalized mineralized area per cell. Values from all z-stack images for each hydrogel were averaged to provide a mean normalized positive area for the whole hydrogel.

Statistical analysis

All data are presented as mean ± standard error of measurement. Statistical testing was carried out using ordinary

one-way (Figs. 1, 6, and 7) and two-way analysis of variance (ANOVA) (Figs. 2, 3, 5, and 8), and repeated-measures two-way ANOVA (Fig. 2B), with Tukey *post hoc* analysis for ANOVA when indicated. Analyses were performed using Prism software (GraphPad). Values of $p < 0.05$ were considered statistically significant.

Experiment

PEG hydrogel formation

PEG hydrogels were formed using norbornene-functionalized PEG macromers and either a nondegradable, dithiol-functionalized PEG crosslinker (ND) or a bis-cysteine peptide crosslinker (MMP) containing the sequence GPQGIWGQ, which is cleaved by a wide range of PDLC-secreted MMPs (Fig. 1A–C).[38,39] We have previously shown that *in vitro* bulk degradation of PEG hydrogels crosslinked with this MMP-degradable peptide occurs primarily in response to enzymatic activity, with minimal hydrolytic cleavage of the ester group linking PEG arms to norbornene moieties.[29] The linear cell-binding peptide ligand RGD (or a Scr noncell-binding peptide [RDG], Scr) was included at a 2 mM concentration to allow PDLC binding to the hydrogel scaffold through integrins αvβ3 and α5β1.[40,41]

Compressive testing showed that all hydrogel compositions had a similar elastic modulus (~10 kPa), indicating a similar degree of crosslinking within each hydrogel (Fig. 1D). Mesh sizes, which are an estimate of the distance between polymer chains, were comparable across conditions (~20 nm) (Fig. 1E) suggesting similar diffusive properties for each hydrogel composition.

PDLC culture and characterization

PDLCs were isolated from the extracted third molars of a single human subject (male, 31 years old) and expanded to passage 3 before characterization and encapsulation in hydrogels. Culture-expanded PDLCs showed surface marker expression patterns typical for mesenchymal cells (Supplementary Fig. S1). The majority of PDLCs were positive for CD146 (94.8%), whereas few (3.5%) were STRO-1 positive (Supplementary Fig. S1). PDLCs demonstrated differentiation potential, forming calcium nodules or lipid droplets after 4 weeks in osteogenic/cementogenic (inductive) or adipogenic culture media. ALP positive cells were present during culture and increased in number over time (Supplementary Fig. S1).

Viability, morphology, and proliferation of encapsulated PDLCs

The viability, spreading, and proliferation of PDLCs within PEG hydrogels was monitored over 3 weeks (Fig. 2 and Supplementary Fig. S2). Viability was high (>90%) at all time points for PDLCs encapsulated in MMP-degradable hydrogels with the RGD ligand (MMP, RGD) (Fig. 2A) but was significantly lower in all hydrogels with nondegradable crosslinkers (ND, Scr and ND, RGD) and decreased over time in both ND and MMP hydrogels with the Scr peptide RDG (ND, Scr and MMP, Scr) (Fig. 2A). PDLCs encapsulated within ND hydrogels showed minimal spreading throughout the entire culture period regardless of RGD inclusion (Fig. 2B). Spreading was greatest overall for PDLCs in MMP, RGD hydrogels at all time points, whereas PDLCs in MMP, Scr demonstrated an increased aspect

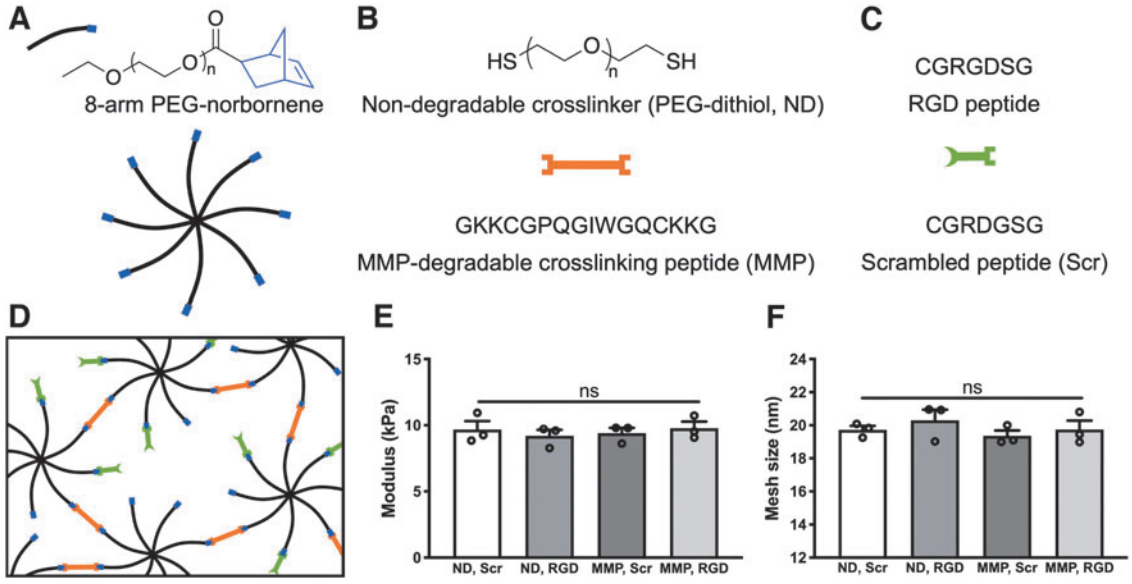

FIG. 1. PEG hydrogels with synthetic peptides replicate key ECM cues. Hydrogels were composed of **(A)** 8-arm PEG-norbornene macromers (8-arm PEG: *black*, norbornene: *blue*), **(B)** nondegradable linear PEG-dithiol (ND) or MMP-degradable peptide (MMP) crosslinkers (*orange*), and **(C)** 2 mM of either RGD or Scr peptide (*green*). **(D)** Polymerization was conducted using the photoinitiator LAP and long-wave ultraviolet light (~5 mW/cm^2, 365 nm for 3 min) with sub-stoichiometric ratio of crosslinker thiol groups to macromer norbornene groups to allow peptide ligand tethering. **(E)** Hydrogel elastic modulus and **(F)** mesh size were similar across all compositions. $N = 3$ hydrogels per condition. Data are shown as individual replicates (*open circles*) with mean (*column*) and standard error of measurement (*error bars*). LAP, lithium phenyl-2,4,6-trimethylbenzoyl phosphinate; ECM, extracellular matrix; PEG, poly(ethylene glycol); MMP, matrix metalloproteinase; ND, nondegradable; Scr, scrambled; ns, not significant.

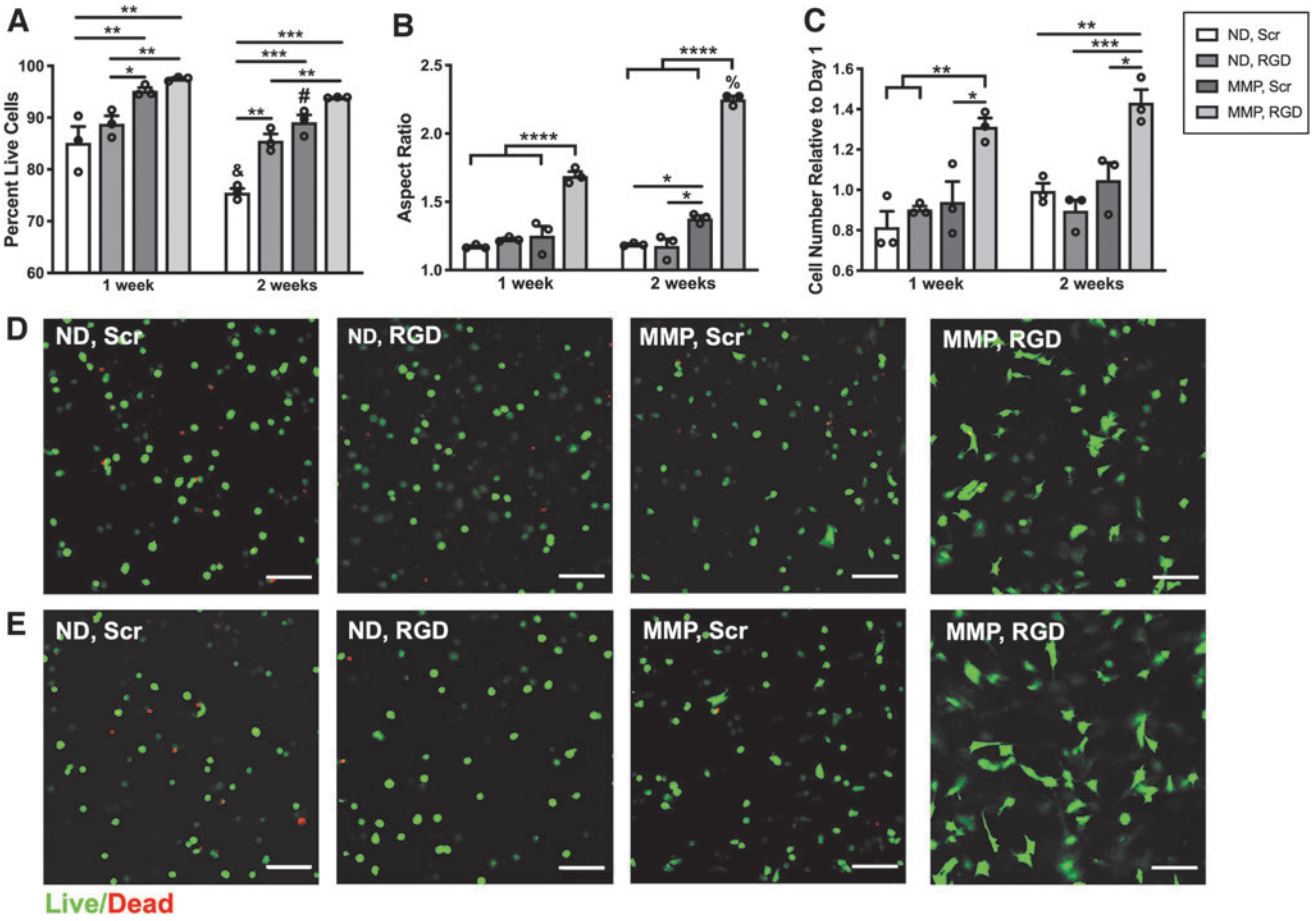

FIG. 2. Both MMP-degradable crosslinker and RGD ligand are required for maximal PDLC viability, spreading, and proliferation. **(A)** PDLC viability was measured by staining live and dead cells and quantifying live cell versus total cell number from confocal images using ImageJ. **(B)** Aspect ratio was quantified using ImageJ analysis of calcein-stained live cells. **(C)** PDLC proliferation was quantified after culturing each hydrogel in 10% alamarBlue at 24 h, 1 week and 2 weeks after formation. Relative cell number was calculated by normalizing mean fluorescence of the culture medium at 1 and 2 weeks to the mean value at 24 h within each hydrogel group. **(D, E)** Representative cross-sectional (z-plane) images of hydrogels illustrating the presence of dead cells (*red*) and round or spread live cells (*green*) after 1 **(D)** or 2 weeks **(E)** of culture. Scale bar is 100 μm. $N=3$ hydrogels. $^{*}p<0.05$, $^{**}p<0.01$, $^{***}p<0.001$, $^{****}p<0.0001$ for between-group comparisons at 1 or 2 weeks. $^{\#}p<0.05$, $^{\&}p<0.001$, $^{\%}p<0.0001$ for within-group comparisons between 1 and 2 weeks. PDLC, periodontal ligament cell.

ratio compared with ND hydrogels by 2 weeks (Fig. 2B). Differences in PDLC morphology across conditions was confirmed in phalloidin-stained hydrogels imaged at higher power (Supplementary Fig. S2). PDLC metabolic activity, indicative of total cell number, increased consistently over time only in MMP, RGD hydrogels (Fig. 2C). When culture conditions were extended to 3 weeks, PDLCs in MMP, RGD hydrogels maintained >90% viability and a spread morphology (Supplementary Fig. S3).

PDL ECM gene and protein expression

A key role for PDL ECM proteins is structural support of the fibrous PDL and maintenance of the interface between the PDL and mineralized cementum and bone. Expression of *POSTN* and *ASPN*, two genes preferentially expressed within the PDL,[42,43] were elevated in PDLCs within MMP, Scr hydrogels cultured in basal medium, whereas expression in MMP, RGD hydrogels did not deviate from baseline (Fig. 3A, B). When cultured in inductive medium, *POSTN* expression was reduced below baseline levels in all hydrogels with the exception of MMP, RGD hydrogels at 2 weeks, whereas *ASPN* expression was elevated in MMP, Scr hydrogels at both 1 and 2 weeks (Fig. 3F).

Collagen type I is the primary organic component of both the fibrous PDL and mineralized cementum and bone.[2] Expression of *COL1A1* was elevated in both MMP, RGD and MMP, Scr hydrogels cultured in basal medium at 1 and 2 weeks, with significantly higher expression at 2 weeks in MMP, Scr hydrogels (Fig. 3C). *COL1A1* expression was reduced below baseline levels in all hydrogels cultured in inductive medium at 1 week. By 2 weeks, *COL1A1* expression had increased in both MMP groups and was significantly higher in the MMP, RGD hydrogels versus counterparts with Scr peptide (Fig. 3G). *ALPL*, a key gene expressed by differentiated cementoblasts, osteoblasts, and cells within the PDL,[44] followed similar trends for all hydrogels in both culture media conditions (Fig. 3D, H). Expression was depressed in ND hydrogels, but progressively increased in both MMP, RGD and MMP, Scr hydrogels,

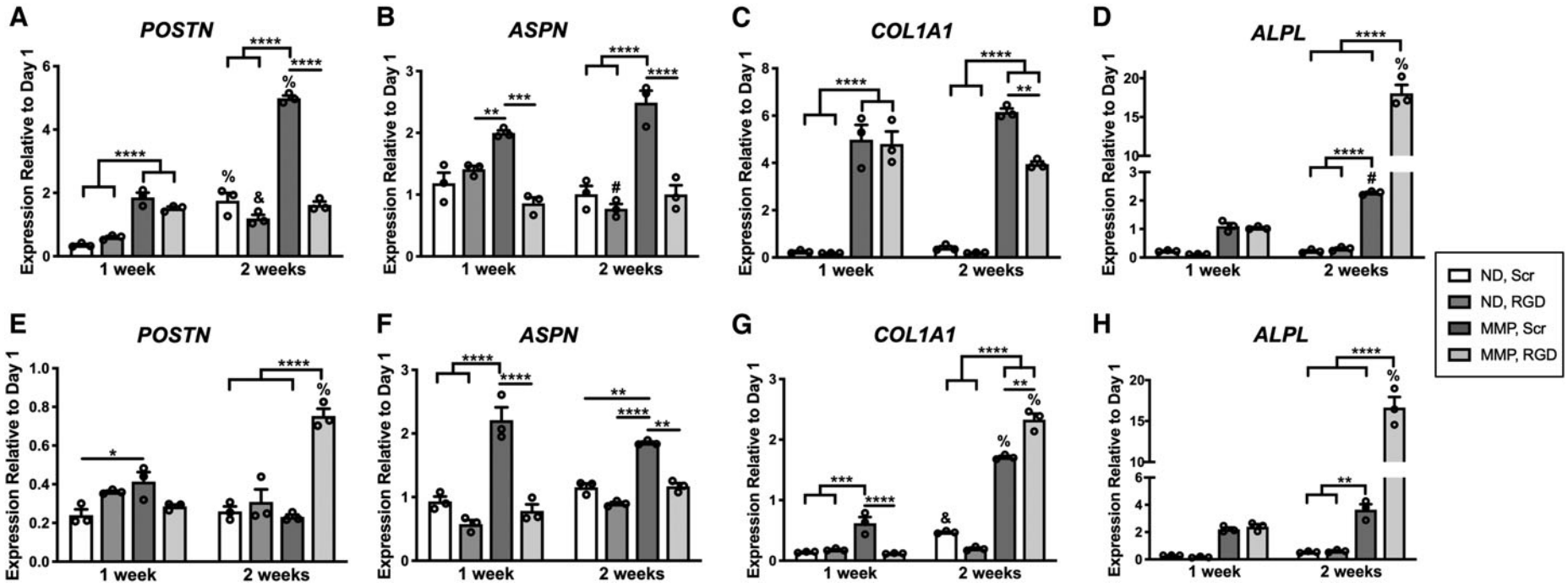

FIG. 3. PDLC ECM gene expression is altered by hydrogel composition, culture media, and culture time. PDLCs were encapsulated in hydrogels and cultured in basal medium **(A–D)** or inductive medium **(E–H)** for 1 or 2 weeks, followed by isolation of mRNA, reverse transcription and quantitative polymerase chain reaction using *RPL32* as the housekeeping gene. Expression levels are reported as fold-change relative to PDLCs isolated from hydrogels postequilibrium swelling at day 1. $^{*}p<0.05$, $^{**}p<0.01$, $^{***}p<0.001$, $^{****}p<0.0001$ for between hydrogel group comparisons at 1 or 2 weeks. $^{\#}p<0.05$, $^{\&}p<0.01$, $^{\%}p<0.0001$ for within hydrogel group comparisons between 1 and 2 weeks.

reaching a nearly 20-fold increase over baseline levels in MMP, RGD hydrogels by 2 weeks of culture in either basal or inductive media (Fig. 3D, H).

Whole hydrogel immunostaining was performed for collagen type 1 (COL1) and periostin (POSTN) after 2 weeks of culture in basal medium (Fig. 4). COL1 was deposited within the hydrogel matrix of MMP, Scr hydrogels up to 10 μm beyond the PLDC border (Fig. 4A), whereas in MMP, RGD hydrogels, extracellular COL1 was present but concentrated at the PDLC periphery (Fig. 4B). Similarly, POSTN was labeled diffusely beyond the immediate borders of PDLCs in MMP, Scr hydrogels and showed limited extracellular expression in MMP, RGD hydrogels (Fig. 4A, B). Extracellular labeling of COL1 was limited to the immediate PDLC periphery within both ND, Scr and ND, RGD hydrogels (Supplementary Fig. S4).

PDLC ALP activity

ALP activity is considered an early marker of PDLC cementogenic/osteogenic differentiation and is required for both cementum and bone formation *in vivo*.[44,45] PDLC ALP activity was elevated six- to eightfold for PDLCs cultured within MMP, Scr and MMP, RGD hydrogels versus both ND hydrogels after either 1 or 2 weeks culture and in either basal or inductive medium (Fig. 5A, C). This distinct increase in ALP activity in MMP hydrogels was confirmed by staining hydrogels for ALP-positive cells (Fig. 5B, D). Of note, ALP activity in MMP, Scr and MMP, RGD hydrogels at 1 or 2 weeks was similar to PDLCs cultured for 2 weeks on tissue culture plates in inductive medium (Fig. 5E). No significant differences were noted when comparing PDLC ALP activity in MMP hydrogels with RGD versus Scr peptide, between 1 or 2 weeks culture time, or in basal versus inductive culture medium (Supplementary Fig. S5).

Cells secrete proteins that contain RGD motifs (e.g., fibronectin) into their ECM with cell binding to ECM proteins and/or hydrogel-tethered RGD ligands activating intracellular pathways that lead to differentiation.[25,46,47] A soluble RGD peptide (sol RGD) was added to hydrogel culture daily for 1 week to block PDLC binding to tethered RGD peptides and/or secreted RGD-containing ECM proteins. Hydrogels were also incubated with a ROCK inhibitor (Y-27632) with or without sol RGD to block actin-mediated intracellular tension over a 1-week period. ALP activity in MMP, Scr hydrogels showed slight, nonsignificant decreases in response to treatment with sol RGD and/or Y-27632 (Fig. 6A), whereas a small, insignificant increase in ALP activity was noted in MMP, RGD hydrogels after treatment with sol RGD. Hydrogel staining with ethidium homodimer-1 and calcein AM indicated that sol RGD treatment led to a significant increase in PDLC aspect ratio in MMP, RGD hydrogels, whereas spreading was reduced in all hydrogels treated with Y-27632 (Fig. 6C–F). No reductions in PDLC viability were noted in response to treatment with sol RGD or Y-27632 (Supplementary Fig. S6).

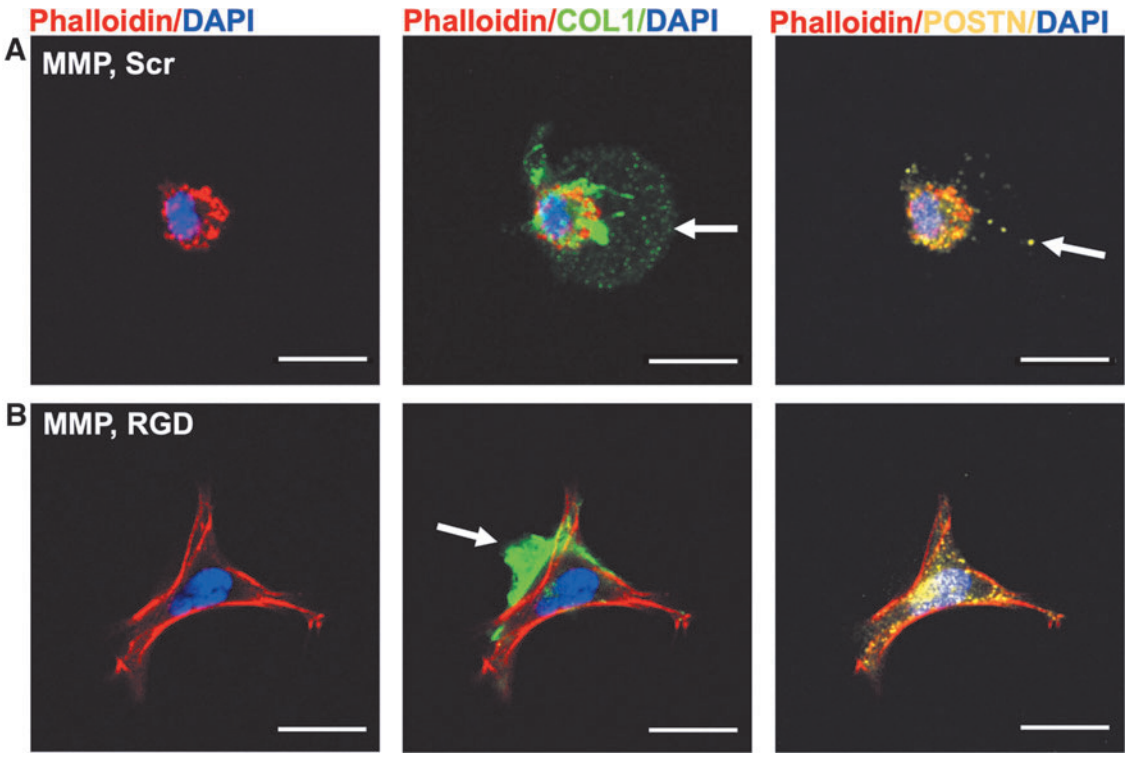

FIG. 4. PDLCs secrete proteins into the ECM of MMP-degradable hydrogels. **(A, B)** Whole hydrogels were fixed and stained for collagen type 1 (COL1, *green*) and periostin (POSTN, *yellow*), the cell cytoskeleton (phalloidin, *red*) and nuclei (DAPI, *blue*) after 2 weeks of culture in basal medium. Representative images of PDLCs in **(A)** MMP, Scr and **(B)** MMP, RGD hydrogels. *White arrow* indicates positively stained protein in the hydrogel ECM. Scale bar is 20 μm. DAPI, 4′,6-diamidino-2-phenylindole.

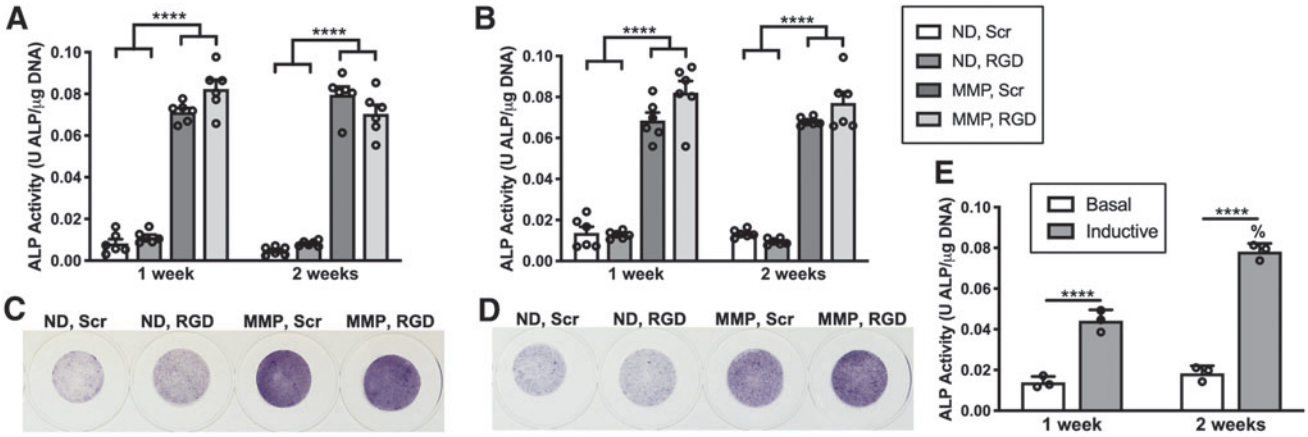

FIG. 5. PDLC ALP activity is elevated in MMP-degradable hydrogels. **(A, B)** ALP activity for hydrogels cultured in basal medium **(A)** and inductive medium **(B)**. ALP activity was calculated by dividing the rate of phosphate substrate (*p*-nitrophenyl phosphate) cleavage by total hydrogel DNA content for each hydrogel using calf intestinal ALP as the standard. **(C, D)** Whole hydrogels were stained with nitro-blue tetrazolium chloride/5-bromo-4-chloro-3′-indolyphosphate p-toluidine salt (NBT/BCIP) to visualize PDLC ALP activity after 2 weeks culture in basal **(C)** or inductive medium **(D)**. $N=6$ hydrogels. **(E)** ALP activity for PDLCs cultured on tissue culture plates in basal or inductive medium. $^{****}p<0.0001$ for between-group comparisons, $^{\%}p<0.0001$ for within-group comparisons. ALP, alkaline phosphatase.

PDLC response to decreased matrix density

Recent studies suggest that changes in cell volume underlie differentiation within three-dimensional matrices.[48,49] To facilitate PDLC volume expansion, the weight percentage of PEG polymer was decreased to create softer, less restrictive matrices with either nondegradable or MMP-degradable crosslinks. Two millimolar tethered RGD peptide was included in all hydrogels to support PDLC viability during extended culture. These soft ND and MMP hydrogels had similar stiffness (~4 kPa) and mesh size (~24 nm) (Supplementary Fig. S7).

The volume and shape (sphericity) of PDLCs was monitored over the first week of culture. PDLCs showed a similar volume within all hydrogels after polymerization and equilibrium swelling (1 day post-encapsulation) (Supplementary Fig. S8). After 1 week, PDLCs in 10 kPa ND, RGD hydrogels remained round, whereas PDLCs in 4 kPa ND, RGD hydrogels showed narrow projections into the hydrogel ECM extending from round cell bodies (Fig. 7D). PDLCs in 10 kPa MMP, RGD hydrogels exhibited a highly spread morphology, whereas PDLCs in 4 kPa, MMP, RGD hydrogels were elongated and spindle-like (Fig. 7D). Overall, PDLC volume was greater in softer versus stiffer and in MMP versus ND hydrogels (Fig. 7A, C). PDLC sphericity, a measurement of three-dimensional cell shape, was lowest overall in 4 kPa MMP, RGD hydrogels, whereas it was similar between soft and stiff ND hydrogels (Fig. 7B).

Metrics of PDLC differentiation were investigated as a function of hydrogel stiffness, degradability, and media composition. ALP activity at 1 week was significantly higher in softer ND and MMP hydrogels versus their stiffer counterparts, with PDLC ALP activity in 4 kPa ND, RGD hydrogels reaching similar levels as stiffer, 10 kPa MMP, RGD hydrogels (Fig. 8A). The 4 kPa MMP, RGD hydrogels supported the highest PDLC ALP activity in both culture media, representing 14- to 18-fold increase over stiff ND hydrogels, and was the only hydrogel composition that showed an increase in ALP activity in response to inductive culture medium (Fig. 8A).

ECM calcium deposition, a late marker of PDLC cementogenic/osteogenic differentiation, was quantified after 3 weeks of culture (Fig. 8B). Minimal matrix mineralization was noted in all hydrogels when cultured in basal medium (Fig. 8C), whereas culture in inductive medium led to increased matrix mineralization in all hydrogels with the exception of 4 kPa MMP, RGD hydrogels (Fig. 8B, D). Stiffer ND and MMP (10 kPa) hydrogels supported greater matrix mineralization versus softer (4 kPa) hydrogels. The 10 kPa, MMP, RGD hydrogels showed the highest mean mineralized area per PDLC in both media conditions (Fig. 8B–D).

Discussion

PDLCs respond to their ECM *in vivo* leading to proliferation, differentiation, and formation of the fibrous PDL and mineralized cementum and bone. Identifying and replicating these ECM cues *in vitro* is critical for understanding the mechanisms underlying these activities, and ultimately for engineering matrices that control PDLC behavior to support periodontal tissue regeneration. This study demonstrates that an MMP-degradable engineered ECM, in particular, supports key metrics of PDLC activity and expression of PDL ECM genes. Integrin binding within the hydrogel matrix, enabled by the RGD peptide, sustains PDLC viability and proliferation when coupled with an MMP-degradable matrix and leads to increased mineral deposition by PDLCs within the synthetic ECM when cultured with pro-mineralization media components. These findings parallel outcomes for BMSCs within similar covalently crosslinked hydrogels where MMP degradability was required for encapsulated BMSCs to spread[50] and to respond to soluble cues from culture media and undergo osteogenic differentiation.[24,25] Although PDLCs show similar *in vitro* plasticity

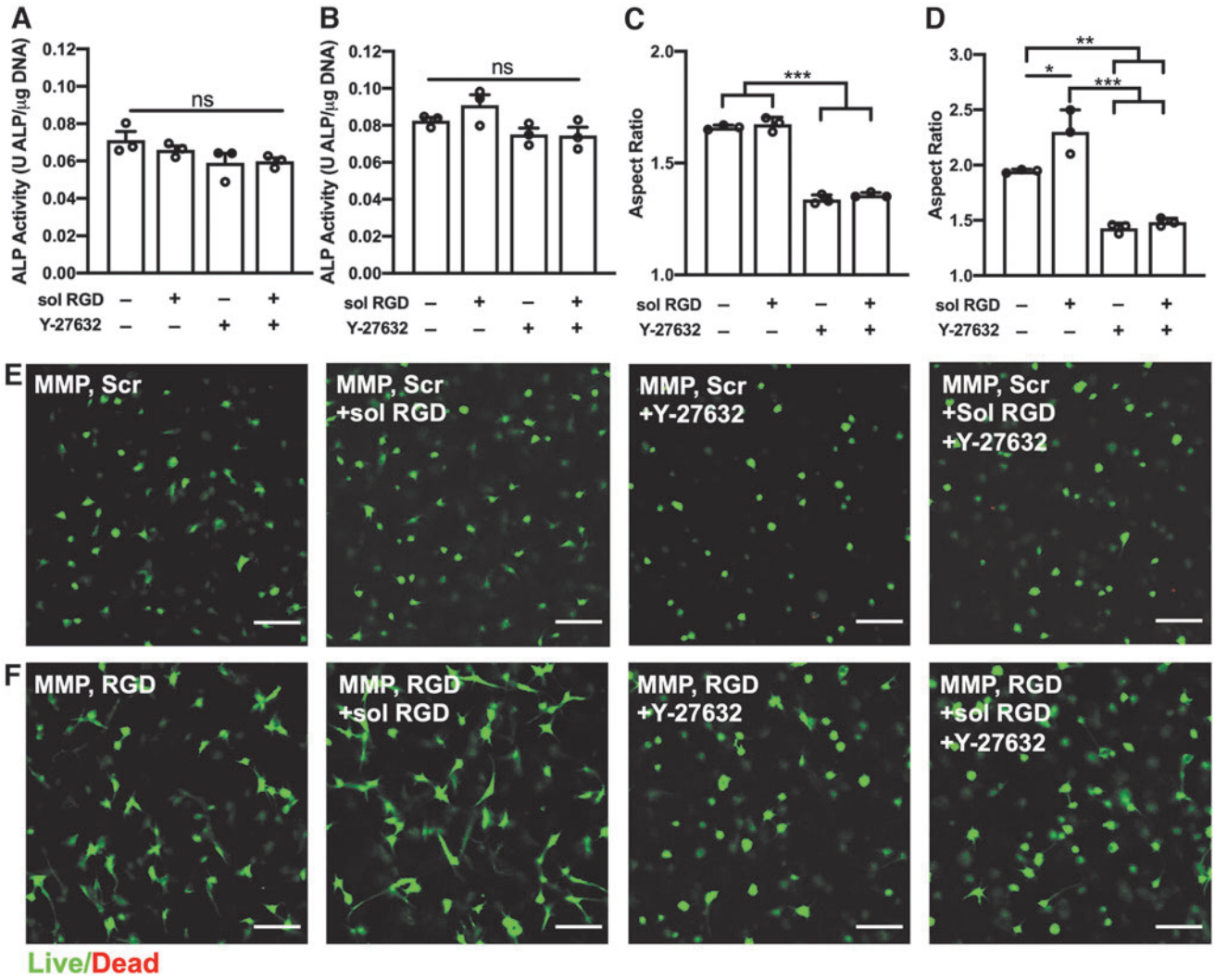

FIG. 6. Treatment with sol RGD and/or rho-associated protein kinase inhibitor Y-27632 alter encapsulated PDLC morphology but not ALP activity. **(A, B)** ALP activity for MMP, Scr **(A)** and MMP, RGD **(B)** hydrogels cultured in basal medium with or without 0.5 mM sol RGD and/or 10 μm Y-27632. **(C, D)** Aspect ratios in MMP, Scr **(C)** and MMP, RGD **(D)** hydrogels. **(E, F)** Representative cross-sectional (z-plane) images of calcein AM and ethidium homodimer 1 stained PDLCs in MMP, Scr **(E)** and MMP, RGD **(F)** hydrogels. $*p<0.05$, $**p<0.01$, $***p<0.001$. Scale bar is 100 μm. $N=3$ hydrogels. sol RGD, soluble RGD.

as BMSCs during conventional culture on plastic plates, they retain distinct properties after culture and transplantation.[12,16] Our findings here show that PDLCs also show a unique response to three-dimensional culture in this hydrogel ECM, acquiring elevated ALP activity in soft and/or enzymatically degradable hydrogels regardless of soluble media cues.

The PDL remains unmineralized in healthy, homeostatic conditions.[51] PDL ECM proteins play a complex role in both the maintenance of the unmineralized state of the PDL and the formation and remodeling of mineralized tissues (bone and/or cementum) at the PDL periphery. Asporin (*ASPN*), previously referred to as periodontal ligament-associated protein-1 (*PLAP-1*), is preferentially expressed in the PDL rather than mineralized cementum and bone and may act as a negative regulator of PDL mineralization.[43,52] Periostin is an matricellular protein, binding fibronectin and other ECM proteins and regulating collagen fibrillogenesis.[53,54] *POSTN* is expressed by fibroblasts throughout the PDL, similar to *ASPN*, but rather than inhibiting osteogenic differentiation, may support PDLC differentiation through PDLC-integrin αvβ3 interactions.[55] In this study, PDLC expression of both *ASPN* and *POSTN* was elevated within MMP-degradable hydrogels without the RGD ligand (MMP, Scr) during culture in basal medium (Fig. 3). *COL1A1* expression was also elevated in MMP, Scr hydrogels, and immunostaining of the hydrogel matrix indicated that both collagen 1 and periostin were deposited by PDLCs within the space degraded by MMPs (Fig. 4). These findings together suggest that PDLC cultured within enzymatically degradable hydrogels without additional ECM cues (integrin binding peptides, soluble culture media cues) may acquire PDL fibroblast characteristics.

The presence of the RGD ligand in MMP-degradable hydrogels resulted in *ASPN* or *POSTN* expression remaining at or below baseline levels together with elevated *COL1A1* and *ALPL* expression in both basal and inductive (cementogenic/osteogenic) media. In particular, the

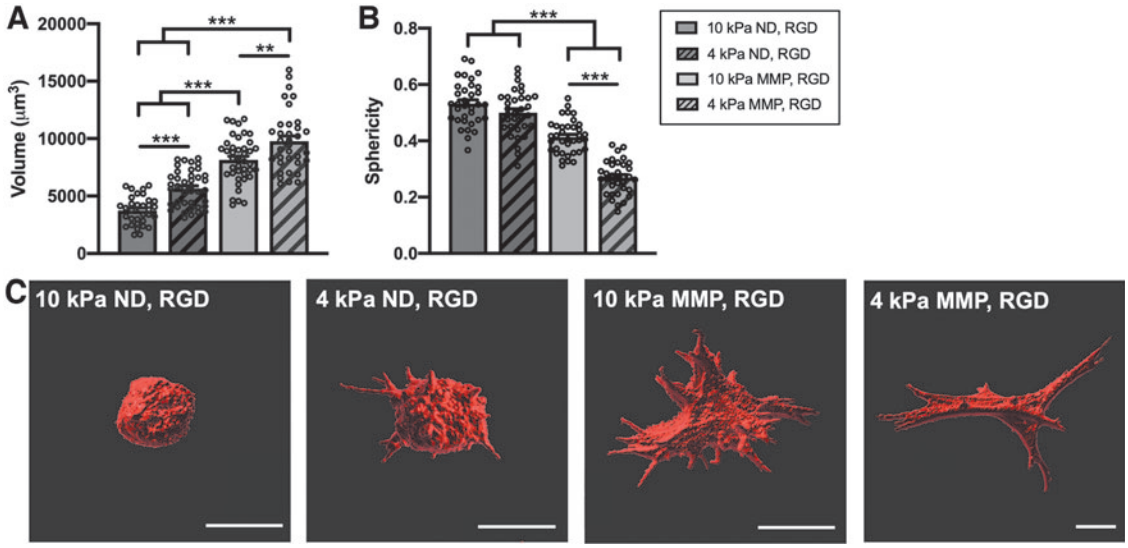

FIG. 7. PDLC volume and shape are affected by hydrogel stiffness and degradability. **(A)** Volume and **(B)** sphericity of PDLCs encapsulated in soft (4 kPa) or stiff (10 kPa) hydrogels with ND or MMP-degradable crosslinkers and RGD ligand and cultured for 1 week in basal medium. **(C)** Representative three-dimensional surface renderings of individual PDLCs within each hydrogel composition. Scale bar is 20 μm. $N = 3$ hydrogels. Symbols indicate measurements for individual cells (≥10 cells/hydrogel). $^{**}p < 0.01$, $^{***}p < 0.001$.

nearly 20-fold increase in *ALPL* expression in both media conditions suggested the initiation of cementogenic/osteogenic differentiation independent of culture media cues. However, PDLC enzymatic ALP activity was found to be a function of MMP degradability with little contribution by RGD or inductive culture medium in stiffness-matched hydrogels (Fig. 5). Furthermore, blocking PDLC–matrix binding and/or intracellular mechanical tension had minimal effect on PDLC ALP activity despite significant changes in cell shape (Fig. 6). Instead, elevated PDLC ALP activity was associated with increased PDLC volume which occurred subsequent to degradation of surrounding peptide crosslinkers in stiffer MMP-degradable hydrogels or by an increase in hydrogel mesh size in softer nondegradable and MMP-degradable hydrogels (Figs. 7 and 8).

Recent studies also show that volume regulation is a key factor underlying differentiation of multipotent cells within hydrogel matrices. BMSCs cultured within viscoelastic alginate hydrogels showed volume expansion resulting from faster hydrogel stress relaxation or decreased osmotic pressure that promoted RUNX2 nuclear localization and ALP activity.[48] A similar relationship between cell volume and osteogenic differentiation was found for adipose tissue-derived stromal cells in elastic gelatin methacryloyl hydrogels; cell volume and RUNX2 expression increased as hydrogel crosslinking and matrix stiffness decreased.[49] Furthermore, in stiffness-matched hyaluronic acid hydrogels, BMSC YAP/TAZ nuclear localization was increased in parallel with cell volume when BMSCs were cultured in the presence of MMP-degradable versus nondegradable crosslinks.[56]

Although PDLC ALP activity was increased in softer PEG hydrogels regardless of degradability, matrix mineralization was reduced compared with stiffer hydrogels (Fig. 8). This opposing effect of ECM cues for fostering PDLC ALP activity versus matrix mineralization may be due to a number of factors. PDLC ALP activity may not be a reliable sign of early cementogenic/osteogenic differentiation within this synthetic ECM. As PDLCs express *ALPL* and show endogenous ALP activity *in vivo*,[44,57] the increased ALP activity in less restrictive hydrogels may represent reaching a ''basal'' level lost during PDLC isolation and expansion,[58] rather than an early indicator of cementogenic/osteogenic differentiation. It is also possible that the hydrogel ECM provided a poor pericellular environment for PDLC-mediated matrix mineralization. Biomineralization of collagen fibrils is promoted within environments containing low pyrophosphate to phosphate ratios (a function of ALP activity) and the presence of pro-mineralization proteins (e.g., BSP and DMP1).[59,60] Although collagen was deposited in these hydrogels (Fig. 4 and Supplementary Fig. S4), the quantity and quality may have been insufficient for nucleation of hydroxyapatite despite elevated PDLC ALP activity. This shortcoming may have been magnified in softer hydrogels that lacked additional polymer structure to support collagen deposition and organization. Quantification of PDLC collagen production in response to changes in matrix density and/or integrin binding may provide additional insight on the interplay between scaffold properties and PDLC matrix mineralization. PDLC production of ECM proteins that promote or inhibit mineralization is also likely to occur in response to matrix cues. Further studies on these factors together with identification of the intracellular pathways associated with increased PDLC ALP activity, are required to better understand ECM-mediated PDLC differentiation.

Although not explored in this study, the concentration and identity of peptide ligands within hydrogel ECMs can be altered to regulate cell–integrin interactions and subsequent cell function. Other *in vitro* studies have demonstrated that PDLCs undergo cementogenic/osteogenic differentiation

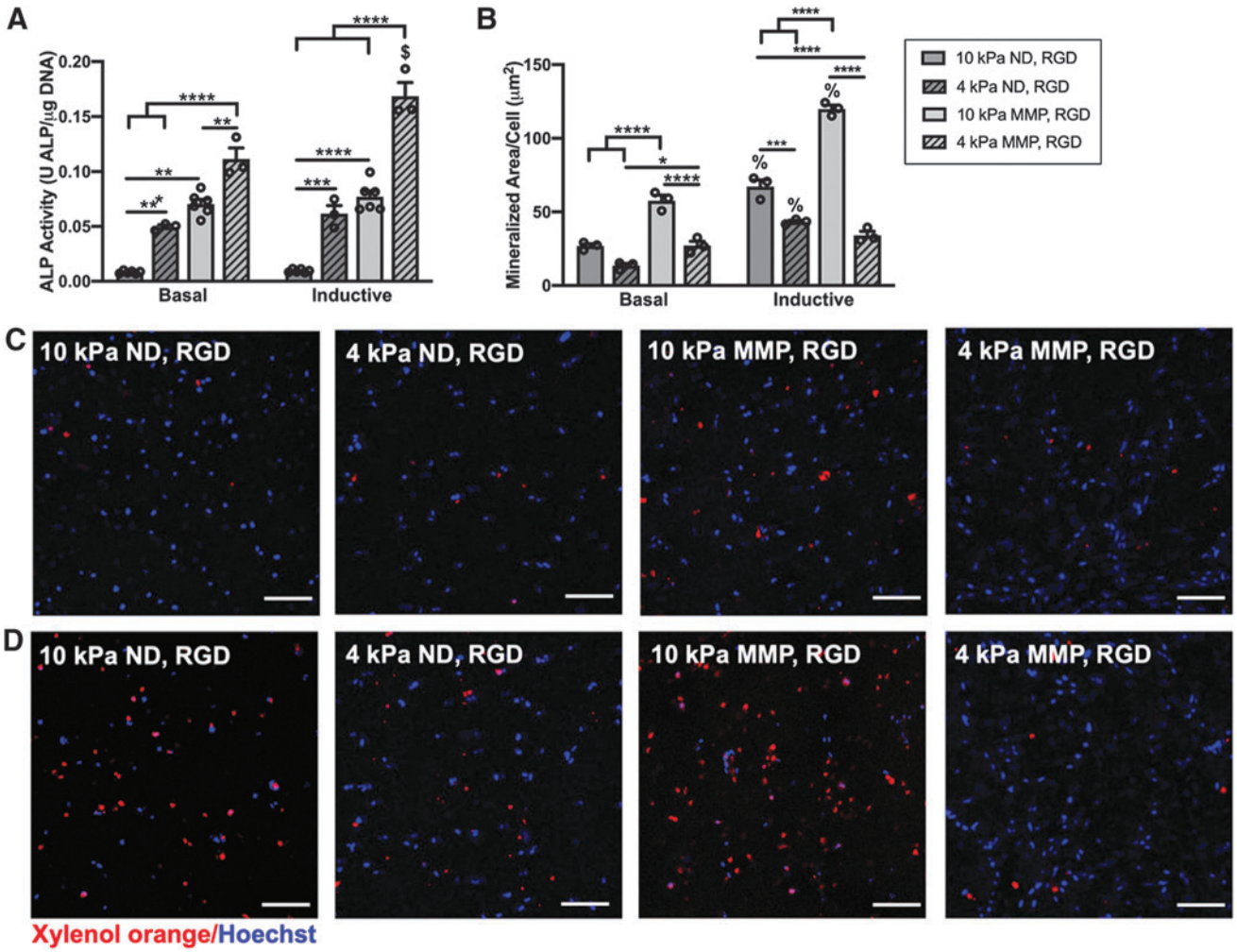

FIG. 8. PDLC ALP activity and matrix mineralization are differentially regulated by hydrogel stiffness and degradability. **(A)** ALP activity after 1 week and **(B)** mean mineralized area per PDLC after 3 weeks culture in basal or inductive medium. **(C, D)** Representative maximum intensity projection confocal images of xylenol orange-labeled calcium deposits (*red*) and Hoechst 33342-labeled PDLC nuclei in hydrogels cultured in basal medium **(C)** or inductive medium **(D)**. Scale bar is 100 μm. $N = 3–6$ hydrogels. $^{*}p < 0.05$, $^{**}p < 0.01$, $^{***}p < 0.001$, $^{****}p < 0.0001$ for between-group comparisons, $^{\$}p < 0.001$, $^{\%}p < 0.0001$ for within-group comparisons for basal versus inductive medium.

after activation of ECM-binding integrins (i.e., α5β1, αvβ3) and subsequent intracellular mechanotransduction.[55,61] Hydrogel encapsulated cells show a dose-dependent response to RGD and other integrin-binding peptides.[62,63] Furthermore, introduction of peptides that mimic cell binding to collagen (through integrin α2β1 binding the GFOGER motif)[64] or laminin (through integrins binding YIGSR or IKVAV motifs)[65,66] can differentially activate intracellular signaling pathways. Peptide-based integrin activation also varies based on the density and degradability of the hydrogel matrix.[67,68] Thus, presentation of peptide cues that better or selectively engage PDLC integrins will also require careful tuning of matrix mechanical properties to ensure enhanced control over phenotype.

Conclusions

Overall, the results of this study indicate key roles for an enzymatically degradable matrix, cell-binding ligands and matrix density in controlling PDLC activity within a synthetic PDL ECM. Inclusion of MMP-degradable hydrogel crosslinks supported expression of PDL ECM genes while maximal PDLC viability and proliferation required both MMP degradability and integrin interactions. ALP activity was elevated in MMP-degradable hydrogels regardless of the inclusion of the RGD ligand or inductive culture medium. Further increase in ALP activity occurred when matrix density was reduced and was associated with PDLC volume expansion. In contrast, PDLC-mediated matrix mineralization was maximized in stiffer, MMP-degradable hydrogels and required the presence of cementogenic/osteogenic culture medium. Balancing the presentation of ECM cues to further control PDLC activity and identifying the *in vivo* implications remains an important challenge for future investigations.

Authors' Contributions

D.F. and D.S.W.B conception and design, D.F. and T.N. collection of data, D.F. and D.S.W.B. analysis and interpretation of data, D.F., T.N. and D.S.W.B. final approval of the manuscript, D.S.W.B.: obtaining of funding.

Disclosure Statement

No competing financial interests exist.

Funding Information

Funding for this research was provided by National Institutes of Health R01AR064200 and P30AR069655.

Supplementary Material

Supplementary Figure S1
Supplementary Figure S2
Supplementary Figure S3
Supplementary Figure S4
Supplementary Figure S5
Supplementary Figure S6
Supplementary Figure S7
Supplementary Figure S8
Supplementary Table S1
Supplementary Table S2

References

1. Ho, S.P., Kurylo, M.P., Fong, T.K., *et al.* The biomechanical characteristics of the bone-periodontal ligament-cementum complex. Biomaterials **31,** 6635, 2010.
2. Nanci, A., and Ten Cate, A.R. Ten Cate's Oral Histology: Development, Structure, and Function. St. Louis, MO: Elsevier, 2013.
3. McCulloch, C.A. Progenitor cell populations in the periodontal ligament of mice. Anat Rec **211,** 258, 1985.
4. Chen, S.C., Marino, V., Gronthos, S., and Bartold, P.M. Location of putative stem cells in human periodontal ligament. J Periodontal Res **41,** 547, 2006.
5. Roguljic, H., Matthews, B.G., Yang, W., Cvija, H., Mina, M., and Kalajzic, I. In vivo identification of periodontal progenitor cells. J Dent Res **92,** 709, 2013.
6. Pitaru, S., Narayanan, A.S., Etikala, A., and Treves-Manusevitz, S. Periodontal stem cells: a historical background and current perspectives. Curr Oral Health Rep **1,** 26, 2014.
7. Smith, P.C., Martínez, C., Martínez, J., and McCulloch, C.A. Role of fibroblast populations in periodontal wound healing and tissue remodeling. Front Physiol **10,** 270, 2019.
8. Kinane, D.F., Stathopoulou, P.G., and Papapanou, P.N. Periodontal diseases. Nat Rev Dis Primers **3,** 17038, 2017.
9. Villar, C.C., and Cochran, D.L. Regeneration of periodontal tissues: guided tissue regeneration. Dent Clin North Am **54,** 73, 2010.
10. Susin, C., and Wikesjö, U.M.E. Regenerative periodontal therapy: 30 Years of lessons learned and unlearned. Periodontol 2000 **62,** 232, 2013.
11. Vaquette, C., Pilipchuk, S.P., Bartold, P.M., Hutmacher, D.W., Giannobile, W.V., and Ivanovski, S. Tissue engineered constructs for periodontal regeneration: current status and future perspectives. Adv Healthc Mater **7,** e1800457, 2018.
12. Seo, B.M., Miura, M., Gronthos, S., *et al.* Investigation of multipotent postnatal stem cells from human periodontal ligament. Lancet **364,** 149, 2004.
13. Menicanin, D., Mrozik, K.M., Wada, N., *et al.* Periodontal-ligament-derived stem cells exhibit the capacity for long-term survival, self-renewal, and regeneration of multiple tissue types in vivo. Stem Cells Dev **23,** 1001, 2014.
14. Lei, M., Li, K., Li, B., Gao, L.-N., Chen, F.-M., and Jin, Y. Mesenchymal stem cell characteristics of dental pulp and periodontal ligament stem cells after in vivo transplantation. Biomaterials **35,** 6332, 2014.
15. Bright, R., Hynes, K., Gronthos, S., and Bartold, P.M. Periodontal ligament-derived cells for periodontal regeneration in animal models: a systematic review. J Periodontal Res **50,** 160, 2015.
16. Dan, H., Vaquette, C., Fisher, A.G., *et al.* The influence of cellular source on periodontal regeneration using calcium phosphate coated polycaprolactone scaffold supported cell sheets. Biomaterials **35,** 113, 2014.
17. Tsumanuma, Y., Iwata, T., Washio, K., *et al.* Comparison of different tissue-derived stem cell sheets for periodontal regeneration in a canine 1-wall defect model. Biomaterials **32,** 5819, 2011.
18. Nunez, J., Vignoletti, F., Caffesse, R.G., and Sanz, M. Cellular therapy in periodontal regeneration. Periodontol 2000 **79,** 107, 2019.
19. Xu, X.-Y., Li, X., Wang, J., He, X.-T., Sun, H.-H., and Chen, F.-M. Concise review: periodontal tissue regeneration using stem cells: strategies and translational considerations. Stem Cells Transl Med **8,** 392, 2019.
20. Bartold, P.M., McCulloch, C.A., Narayanan, A.S., and Pitaru, S. Tissue engineering: a new paradigm for periodontal regeneration based on molecular and cell biology. Periodontol 2000 **24,** 253, 2000.
21. Luan, X., Dangaria, S., Ito, Y., *et al.* Neural crest lineage segregation: a blueprint for periodontal regeneration. J Dent Res **88,** 781, 2009.
22. Bryant, S.J., and Vernerey, F.J. Programmable hydrogels for cell encapsulation and neo-tissue growth to enable personalized tissue engineering. Adv Healthc Mater **7**, [Epub ahead ofprint]; DOI: 10.1002/adhm.201700605, 2018.
23. Thomas, D., O'Brien, T., and Pandit, A. Toward customized extracellular niche engineering: progress in cell-entrapment technologies. Adv Mater **30,** [Epub ahead of print]; DOI: 10.1002/adma.201703948,2018.
24. Anderson, S.B., Lin, C.C., Kuntzler, D.V., and Anseth, K.S. The performance of human mesenchymal stem cells encapsulated in cell-degradable polymer-peptide hydrogels. Biomaterials **32,** 3564, 2011.
25. Khetan, S., Guvendiren, M., Legant, W.R., Cohen, D.M., Chen, C.S., and Burdick, J.A. Degradation-mediated cellular traction directs stem cell fate in covalently crosslinked three-dimensional hydrogels. Nat Mater **12,** 458, 2013.
26. Clark, A.Y., Martin, K.E., García, J.R., *et al.* Integrin-specific hydrogels modulate transplanted human bone marrow-derived mesenchymal stem cell survival, engraftment, and reparative activities. Nat Commun **11,** 114, 2020.
27. Kyburz, K.A., and Anseth, K.S. Synthetic mimics of the extracellular matrix: how simple is complex enough? Ann Biomed Eng **43,** 489, 2015.
28. Fairbanks, B.D., Schwartz, M.P., Halevi, A.E., Nuttelman, C.R., Bowman, C.N., and Anseth, K.S. A versatile synthetic extracellular matrix mimic via thiol-norbornene photopolymerization. Adv Mater **21,** 5005, 2009.
29. Shubin, A.D., Felong, T.J., Schutrum, B.E., Joe, D.S.L., Ovitt, C.E., and Benoit, D.S.W. Encapsulation of primary salivary gland cells in enzymatically degradable poly(ethylene glycol) hydrogels promotes acinar cell characteristics. Acta Biomater **50,** 437, 2017.

30. Anthis, N.J., and Clore, G.M. Sequence-specific determination of protein and peptide concentrations by absorbance at 205 nm. Protein Sci **22,** 851, 2013.
31. Fairbanks, B.D., Schwartz, M.P., Bowman, C.N., and Anseth, K.S. Photoinitiated polymerization of peg-diacrylate with lithium phenyl-2,4,6-trimethylbenzoylphosphinate: polymerization rate and cytocompatibility. Biomaterials **30,** 6702, 2009.
32. Van Hove, A.H., Wilson, B.D., and Benoit, D.S. Microwave-assisted functionalization of poly(ethylene glycol) and on-resin peptides for use in chain polymerizations and hydrogel formation. J Vis Exp e50890, 2013.
33. Mrozik, K., Gronthos, S., Shi, S., and Bartold, P.M. A method to isolate, purify, and characterize human periodontal ligament stem cells. Methods Mol Biol **1537,** 413, 2017.
34. Pfaffl, M.W. A new mathematical model for relative quantification in real-time RT-PCR. Nucleic Acids Res **29,** e45,2001.
35. Dean, R.L. Kinetic studies with alkaline phosphatase in the presence and absence of inhibitors and divalent cations. Biochem Mol Biol Educ **30,** 401, 2002.
36. Wang, Y.-H., Liu, Y., Maye, P., and Rowe, D.W. Examination of mineralized nodule formation in living osteoblastic cultures using fluorescent dyes. Biotechnol Prog **22,** 1697, 2006.
37. Moshaverinia, A., Chen, C., Xu, X., *et al.* Bone regeneration potential of stem cells derived from periodontal ligament or gingival tissue sources encapsulated in RGD-modified alginate scaffold. Tissue Eng Part A **20,** 611, 2014.
38. Nagase, H., and Fields, G.B. Human matrix metalloproteinase specificity studies using collagen sequence-based synthetic peptides. Biopolymers **40,** 399, 1996.
39. Steffensen, B., Häkkinen, L., and Larjava, H. Proteolytic events of wound-healing—coordinated interactions among matrix metalloproteinases (MMPs), integrins, and extracellular matrix molecules. Crit Rev Oral Biol Med **12,** 373, 2001.
40. Grzesik, W.J., Ivanov, B., Robey, F.A., Southerland, J., and Yamauchi, M. Synthetic integrin-binding peptides promote adhesion and proliferation of human periodontal ligament cells in vitro. J Dent Res **77,** 1606, 1998.
41. Hersel, U., Dahmen, C., and Kessler, H. RGD modified polymers: biomaterials for stimulated cell adhesion and beyond. Biomaterials **24,** 4385, 2003.
42. Rios, H., Koushik, S.V., Wang, H., *et al.* Periostin null mice exhibit dwarfism, incisor enamel defects, and an early-onset periodontal disease-like phenotype. Mol Cell Biol **25,** 11131, 2005.
43. Yamada, S., Tomoeda, M., Ozawa, Y., *et al.* Plap-1/asporin, a novel negative regulator of periodontal ligament mineralization. J Biol Chem **282,** 23070, 2007.
44. Zweifler, L.E., Patel, M.K., Nociti, F.H., Jr., *et al.* Counter-regulatory phosphatases Tnap and Npp1 temporally regulate tooth root cementogenesis. Int J Oral Sci **7,** 27, 2014.
45. Golub, E.E., and Boesze-Battaglia, K. The role of alkaline phosphatase in mineralization. Curr Opin Orthop **18,** 444, 2007.
46. Loebel, C., Mauck, R.L., and Burdick, J.A. Local nascent protein deposition and remodelling guide mesenchymal stromal cell mechanosensing and fate in three-dimensional hydrogels. Nat Mater **18,** 883, 2019.
47. Ferreira, S.A., Motwani, M.S., Faull, P.A., *et al.* Bi-directional cell-pericellular matrix interactions direct stem cell fate. Nat Commun **9,** 4049, 2018.
48. Lee, H.-P., Stowers, R., and Chaudhuri, O. Volume expansion and Trpv4 activation regulate stem cell fate in three-dimensional microenvironments. Nat Commun **10,** 529, 2019.
49. Major, L.G., Holle, A.W., Young, J.L., *et al.* Volume adaptation controls stem cell mechanotransduction. ACS Appl Mater Interfaces **11,** 45520, 2019.
50. Lei, Y., Gojgini, S., Lam, J., and Segura, T. The spreading, migration and proliferation of mouse mesenchymal stem cells cultured inside hyaluronic acid hydrogels. Biomaterials **32,** 39, 2011.
51. Beertsen, W., McCulloch, C.A., and Sodek, J. The periodontal ligament: a unique, multifunctional connective tissue. Periodontol 2000 **13,** 20, 1997.
52. Kajikawa, T., Yamada, S., Tauchi, T., *et al.* Inhibitory effects of Plap-1/asporin on periodontal ligament cells. J Dent Res **93,** 400, 2014.
53. Norris, R.A., Damon, B., Mironov, V., *et al.* Periostin regulates collagen fibrillogenesis and the biomechanical properties of connective tissues. J Cell Biochem **101,** 695, 2007.
54. Kudo, A., and Kii, I. Periostin function in communication with extracellular matrices. J Cell Commun Signal **12,** 301, 2018.
55. Yamada, S., Tauchi, T., Awata, T., *et al.* Characterization of a novel periodontal ligament-specific periostin isoform. J Dent Res **93,** 891, 2014.
56. Caliari, S.R., Vega, S.L., Kwon, M., Soulas, E.M., and Burdick, J.A. Dimensionality and spreading influence Msc Yap/Taz signaling in hydrogel environments. Biomaterials **103,** 314, 2016.
57. Groeneveld, M.C., Van den Bos, T., Everts, V., and Beertsen, W. Cell-bound and extracellular matrix-associated alkaline phosphatase activity in rat periodontal ligament. J Periodontal Res **31,** 73, 1996.
58. Lallier, T.E., and Spencer, A. Use of microarrays to find novel regulators of periodontal ligament fibroblast differentiation. Cell Tissue Res **327,** 93, 2007.
59. Reznikov, N., Steele, J.A.M., Fratzl, P., and Stevens, M.M. A materials science vision of extracellular matrix mineralization. Nat Rev Mater **1,** 16041,2016.
60. George, A., and Veis, A. Phosphorylated proteins and control over apatite nucleation, crystal growth, and inhibition. Chem Rev **108,** 4670, 2008.
61. Wang, H., Li, J., Zhang, X., *et al.* Priming integrin alpha 5 promotes the osteogenic differentiation of human periodontal ligament stem cells due to cytoskeleton and cell cycle changes. J Proteomics **179,** 122, 2018.
62. Yang, F., Williams, C.G., Wang, D.-A., Lee, H., Manson, P.N., and Elisseeff, J. The effect of incorporating RGD adhesive peptide in polyethylene glycol diacrylate hydrogel on osteogenesis of bone marrow stromal cells. Biomaterials **26,** 5991, 2005.
63. Usprech, J., Romero, D.A., Amon, C.H., and Simmons, C.A. Combinatorial screening of 3D biomaterial properties that promote myofibrogenesis for mesenchymal stromal cell-based heart valve tissue engineering. Acta Biomater **58,** 34, 2017.
64. Reyes, C.D., and Garcia, A.J. Alpha2beta1 integrin-specific collagen-mimetic surfaces supporting osteoblastic differentiation. J Biomed Mater Res A **69,** 591, 2004.

65. Weiss, M.S., Bernabé, B.P., Shikanov, A., *et al.* The impact of adhesion peptides within hydrogels on the phenotype and signaling of normal and cancerous mammary epithelial cells. Biomaterials **33,** 3548, 2012.
66. Silva Garcia, J.M., Panitch, A., and Calve, S. Functionalization of hyaluronic acid hydrogels with ECM-derived peptides to control myoblast behavior. Acta Biomater **84,** 169, 2019.
67. Xin, S., Gregory, C.A., and Alge, D.L. Interplay between degradability and integrin signaling on mesenchymal stem cell function within poly(ethylene glycol) based microporous annealed particle hydrogels. Acta Biomater **101,** 227, 2020.
68. Gandavarapu, N.R., Alge, D.L., and Anseth, K.S. Osteogenic differentiation of human mesenchymal stem cells on A5 integrin binding peptide hydrogels is dependent on substrate elasticity. Biomater Sci **2,** 352, 2014.

Address correspondence to:
Danielle S.W. Benoit, PhD
Department of Biomedical Engineering
University of Rochester
308 Robert B. Goergen Hall
Box 271068
Rochester, NY 14627
USA

E-mail: benoit@bme.rochester.edu

Received: September 17, 2020
Accepted: October 23, 2020
Online Publication Date: December 9, 2020